

Li₂S-P₂S₅ Based Solid State Electrolytes for Lithium Ion Battery Applications

James Trevey, Yoon Seok Jung, Se-Hee Lee*

Department of Mechanical Engineering, University of Colorado, Boulder, CO, USA

Sulfide-based Li₂S-P₂S₅ solid state electrolytes were prepared by a high energy ball milling process. Characterization of the xLi₂S-(100-x)P₂S₅ system for 70<x<80 was carried out for both amorphous glass and crystalline glass-ceramic materials by X-ray diffraction and electrochemical methods. Both glass and glass-ceramic electrolytes exhibited high conductivity over 10⁻⁴ S cm⁻¹ at room temperature. Glass-ceramics were proved to have higher stability against lithium metal than respective glass electrolytes. All-solid-state batteries using the glass and glass-ceramic electrolytes were constructed to evaluate the cell performance as a lithium secondary battery. The cell Li/80Li₂S-20P₂S₅ glass/LiCoO₂ performed the best but displayed a large initial irreversible capacity.

Introduction

Research on lithium ion conduction solid electrolytes has increased drastically in recent years due to raised concerns about safety hazards such as solvent leakage and flammability of liquid electrolytes used for commercial lithium-ion batteries^[1]. Solid state electrolytes have been introduced as a remedy to negate safety threats associated with conventional liquid electrolytes. Batteries using a solid state electrolyte are safer to use, do not leak hazardous liquid electrolyte, have a wide selection of compositions, can vary in form design, and have high reliability^[2-4]. Ideally, liquid electrolytes will be replaced by solid state electrolytes that perform similarly without excessive safety issues^[5]. Current research has yet to unveil a solid state electrolyte that can outperform liquid electrolyte. Inferior rate capability, low ionic conductivity, interfacial instability, and low loading of active materials are just a few of the characteristics of solid state batteries that need to be improved before moving towards commercialization.

While melt and quench methods have produced many favorable results over the past decades, high-energy mechanical ball milling is emerging as a new means of producing amorphous materials for solid state electrolytes. Ball milling possesses a favorable feature of directly obtaining fine powders under room temperature operation^[1]. Ball milling produces ultra-fine powders good for achieving high ionic conductivities as well as close contact between electrolyte and electrode materials for solid-state cells. The process of high energy ball milling is a powerful method to prepare amorphous materials and is effective to enlarge the compositional region in which amorphous materials are obtained beyond that of conventional melt-quenching methods^[6]. We have succeeded in preparing Li₂S-P₂S₅ based systems using a high-energy mechanical ball mill technique.

Using modern analysis techniques we have been able to compile a reputable analysis of the [xLi₂S-(100-x)P₂S₅] system for 70<x<80. Sulfide-based glasses containing large amounts of Li₂S are expected to have higher ion conductivities because the Li₂S component generates lithium ion species working as carriers for ion conduction^[6]. Our focus has been on the evaluation of heat treatment of amorphous ball milled powders containing large amounts of Li₂S in the Li-S-P system. Heat treatment of glass samples to

a crystalline glass-ceramic state has shown to increase conductivity [2-4, 7]. All-solid-state lithium batteries were assembled with the glass and glass-ceramic electrolytes and the resulting performances were assessed.

Experimental

Reagent-grade powders of Li_2S (Aldrich, 99.99%) and P_2S_5 (Aldrich, 99.99%) are used as starting materials for mechanical milling. Appropriate concentrations of materials are combined into a plastic vial (Nalgene 125mL) at a net weight of two grams with 50 zirconia balls (5mm diameter) for grinding. High energy ball milling takes place for 20 hours to achieve an amorphous state^[8]. Amorphous ball milled mixtures are cold pressed (8 metric tons) into pellets 13mm in diameter and 1mm thick. Crystalline glass-ceramic samples are formed by baking of pressed pellets on a hot plate at a concentration dependent temperature and time shown in Table I^[9]. After heat treatment, samples are ground with mortar and pestle and re-pelletized. Operations concerning exposed materials were carried out in a glove box filled with dry argon gas and ball milling was performed in an sealed argon environment.

TABLE I. Heat Treatment

Species Content	Time (h)	Temperature (°C)
70 Li_2S -30 P_2S_5	1	360
75 Li_2S -25 P_2S_5	2	300
80 Li_2S -20 P_2S_5	4	240

Characterization

The obtained samples were characterized by use of X-ray diffraction measurements with $\text{Cu-K}\alpha$ radiation. Sample materials were sealed in an airtight aluminum container with beryllium windows and mounted on the X-ray diffractometer (PANalytical, PW3830).

Ionic conductivities were measured by ac impedance spectroscopy (Solartron 1280C) for both glass and glass-ceramic samples. Subsequent to cold pressing samples at 8 metric tons, lithium metal plates are pressed to both sides at 1 metric ton to serve as electrodes. Final sandwiched pellets were pressed into coin cell shells to encapsulate the inert argon atmosphere and make for safe removal from the glove box. The impedance of selected cells was measured from 20 MHz to 100 mHz at room temperature and the conductivity was determined using complex impedance analysis.

The electrochemical stability of the obtained samples was examined using cyclic voltammetry (Arbin BT2000). A triple layer sandwich cell was produced from pressing the working electrode, solid state electrolyte, and counter/reference electrode layers together. The working electrode was comprised of a mixture of acetylene black and the selected solid state electrolyte powder at a ratio of 2:26 by weight respectively, the electrolyte layer was composed of 150 mg of solid state electrolyte powder, and the counter/reference electrode was a plate of lithium foil. The potential sweep was performed in the range of 2.0 to 5.0 V vs. the lithium reference electrode with a scanning rate of 25 $\mu\text{V/s}$.

All-solid-state batteries were prepared with the ball milled electrolytes to observe the cycling performance associated with a given solid state electrolyte. These batteries employed a mixture of LiCoO_2 (4 mg), the solid electrolyte (6 mg), and acetylene black

(0.6 mg) as the positive electrode^[10, 11] and lithium metal as the negative electrode. The battery was constructed by pressing the positive electrode mixture and the solid electrolyte powder together as a double layer pellet at 4.5 tons before pressing the negative electrode onto the pellet at one ton. Galvanostatic charge-discharge cycling was performed between 2.5 and 4.8 V at 50°C using the Arbin BT2000 system.

Results and Discussion

Figure 1 shows the X-ray diffraction (XRD) spectra of the glass and glass-ceramic samples in the composition range $70 < x < 80$ for $[x\text{Li}_2\text{S}-(100-x)\text{P}_2\text{S}_5]$. The broad peaks at 17° and 30° denote the amorphous state of glass samples obtained from high energy ball milling for 20 hours. Sharp diffraction peaks are not observed for concentrations of $x=70$ and $x=75$ glass but are observed for $x=80$ glass electrolyte due to excess Li_2S content in the sample^[12]. From the figure it is concluded that there is no phase change for $x=80$ due to the high Li_2S content raising the crystallization temperature. The diffraction patterns for heat treated samples of $x=70$ and $x=75$ change dramatically. Based on these results, the crystallization temperature can be assumed to be dependent on the concentration of contained species. Individual properties of compounds such as the low melting temperature of P_2S_5 may be a factor in determination of the crystallization temperature. Spectra of amorphous glass and heat treated glass-ceramic samples were obtained via XRD and compared to observe differences in crystallinity.

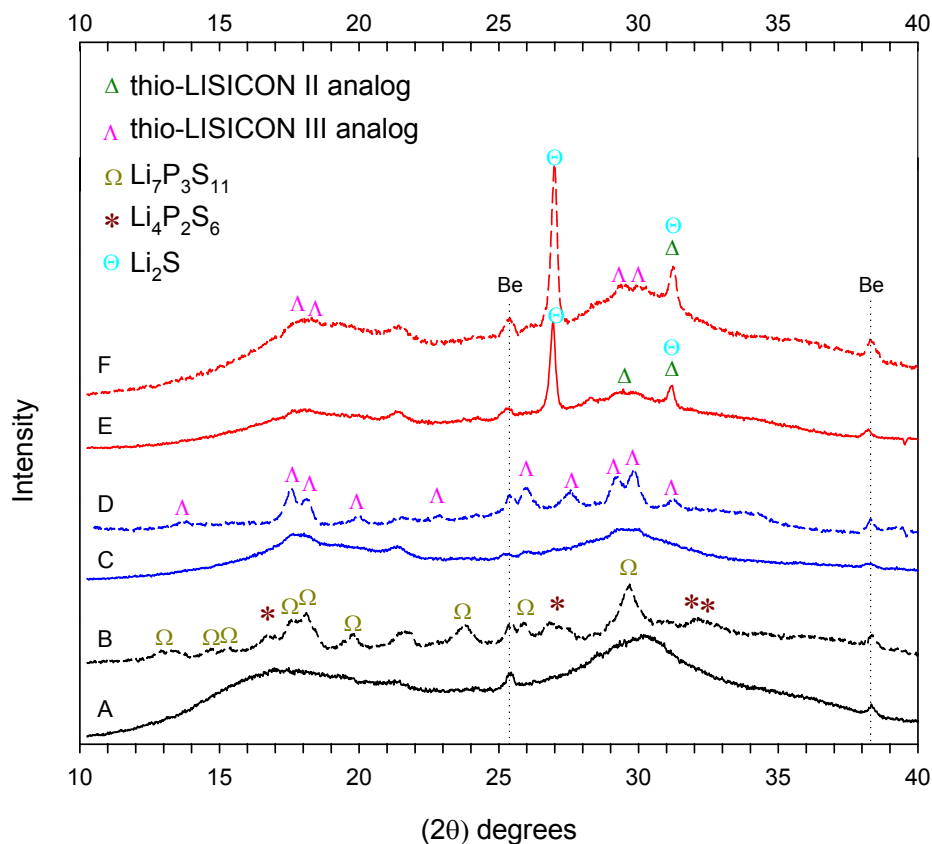


Figure 1. XRD patterns for all tested electrolytes, (A) $x=70$ glass, (B) $x=70$ glass-ceramic, (C) $x=75$ glass, (D) $x=75$ glass-ceramic, (E) $x=80$ glass, and (F) $x=80$ glass-ceramic. Trends observed indicate that for $x=80$ heat treatment has almost no effect on

crystallinity but, for $x=75$ and $x=70$, heat treatment causes a shift from amorphous to crystalline patterns.

Figure 2 shows a conductivity map comparing the conductivity values attained from testing all glass and glass-ceramic solid state electrolytes. Actual values for the ionic conductivity of solid electrolytes are specified in Table II. The increase in conductivity through heat treatment was caused by the formation of new highly conductive crystalline structures. For the lithium-rich $80\text{Li}_2\text{S}-20\text{P}_2\text{S}_5$ glass, enhancement on conductivity by heat treatment of the crystallization temperature was due to formation of a highly conductive crystalline phase analogous to the thio-LISICON phase $\text{Li}_{4-x}\text{Ge}_{1-x}\text{P}_x\text{S}_4$ ($0.6 < x < 0.8$) defined by a unique monoclinic superstructure exhibiting high conductivities over $10^{-3} \text{ S cm}^{-1}$ [13]. While the values for our glass samples are concurrent with previously reported data [9,14], the values we found for our glass-ceramics were consistently lower by one order of magnitude than the values attained by Tatsumisago et al. This disparity between the results could be due to the procedural differences or contamination. Concurrent with Figure 1, there is no significant change in conductivity for $x=80$ as there is no significant change in diffraction pattern between glass and glass-ceramic samples.

TABLE II. Conductivity

Species Content	Amorphous Glass	Heat Treated Glass Ceramic
$70\text{Li}_2\text{S}-30\text{P}_2\text{S}_5$	3.36×10^{-5}	1.39×10^{-4}
$75\text{Li}_2\text{S}-25\text{P}_2\text{S}_5$	9.00×10^{-5}	3.01×10^{-5}
$80\text{Li}_2\text{S}-20\text{P}_2\text{S}_5$	1.43×10^{-4}	1.67×10^{-4}

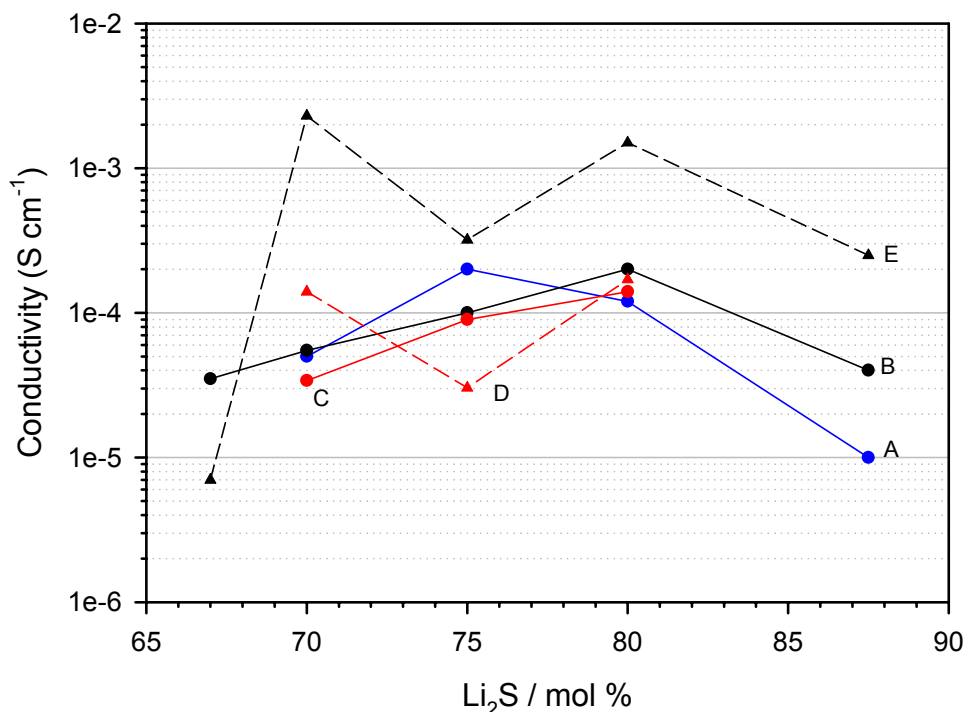


Figure 2. Conductivity map for $[x\text{Li}_2\text{S}-(100-x)\text{P}_2\text{S}_5]$ (mol%) for $70 < x < 80$ (A) glass^[14], (B) glass^[9], (C) Obtained glass, (D) Obtained glass-ceramic, (E) glass-ceramic^[9]. The

trends between [9] and our research are identical while the values differ greatly. This disparity between the results could be due to procedural differences or contamination.

Figure 3 shows stability window for samples tested with acetylene black as the working electrode. Previous research has not paid much attention to the oxidation stability of the $[x\text{Li}_2\text{S}-(100-x)\text{P}_2\text{S}_5]$ solid state electrolyte. Generally, measurement of the electrochemical window is done using Au. This approach however is not accurate for measuring the electrochemical window because the interfacial area between the active powder and the solid state electrolyte is much smaller. In these regards, the acetylene black and solid state electrolyte composite electrode is a far better and more accurate means of measuring the real electrochemical window. In measuring a species electrochemical window, high currents coincide with instability. Since acetylene black cannot be oxidized, higher recorded currents and reduced stability indicate oxidation of the electrolyte. In our case the most favorable electrolytes are $x=75$ glass-ceramic and $x=80$ glass ceramic because they showed the lowest recorded currents. The glass-ceramic electrolytes show a less severe oxidation reaction than the glass electrolytes. We speculate that particle growth during heat treatment results in decreased surface area of the solid state electrolyte. The smaller surface area permits less available material to be oxidized, yielding a better electrochemical window.

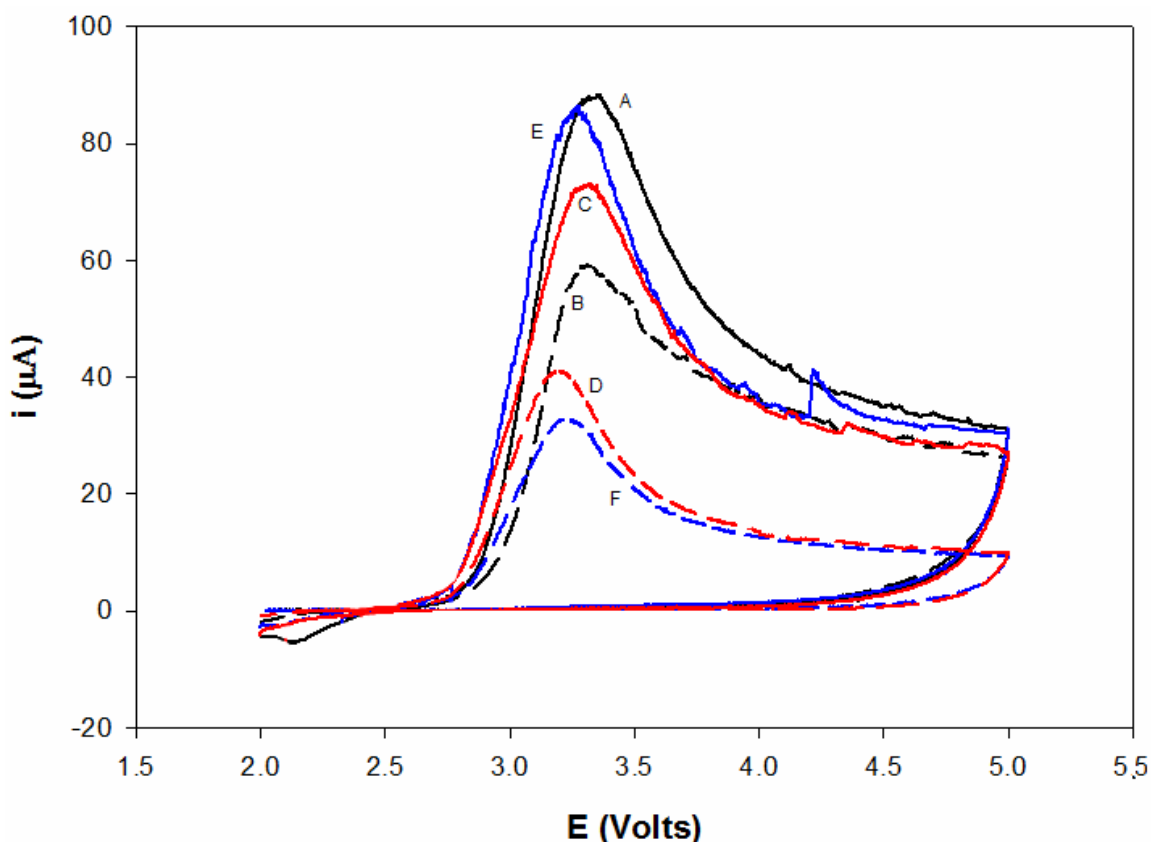


Figure 3. The stability window for the first cycle of tested glass and glass-ceramic samples (A) $x=70$ glass, (B) $x=70$ glass-ceramic, (C) $x=75$ glass, (D) $x=75$ glass-ceramic, (E) $x=80$ glass, and (F) $x=80$ glass-ceramic. Glass-ceramics are shown to be more stable than glass electrolytes. Repeated cycling shows a negligible difference in the stability window.

Figure 4 shows the first charge-discharge curves of the electrochemical cell using lithium metal as the anode, $80\text{Li}_2\text{S}-20\text{P}_2\text{S}_5$ glass as the solid electrolyte, and LiCoO_2 mixed with solid electrolyte powder as the negative electrode. Cells were charged up to 4.8 V and discharged to 2.5 V under the current density of $100 \mu\text{A}/\text{cm}^2$; the conditions of lithium secondary batteries. Lithium ions pass through the electrolyte from the LiCoO_2 to the lithium anode during the charge process and are extracted during discharge. High ionic conductivity of solid electrolytes generally corresponds to improved battery performance^[6]. A large irreversible capacity was observed in the first cycle in all samples using the $[\text{xLi}_2\text{S}-(100-\text{x})\text{P}_2\text{S}_5]$ electrolyte, with $\text{x}=80$ showing the smallest irreversible capacity of the tested solid electrolytes. The increasing irreversibility in Figure 4 is the result of a resistance layer build-up of decomposed solid state electrolyte sulfur compounds. Every cycle causes a larger resistance layer that prevents ionic conduction and reduces the reversible capacity. Initially large irreversible capacities are observed because of low ionic conductivity, but continuously decreasing reversibility in this case points to a resistance layer build up. Further advancement of the $[\text{xLi}_2\text{S}-(100-\text{x})\text{P}_2\text{S}_5]$ solid electrolyte may reduce the irreversible capacity and enhance electrochemical properties for all-solid-state lithium batteries.

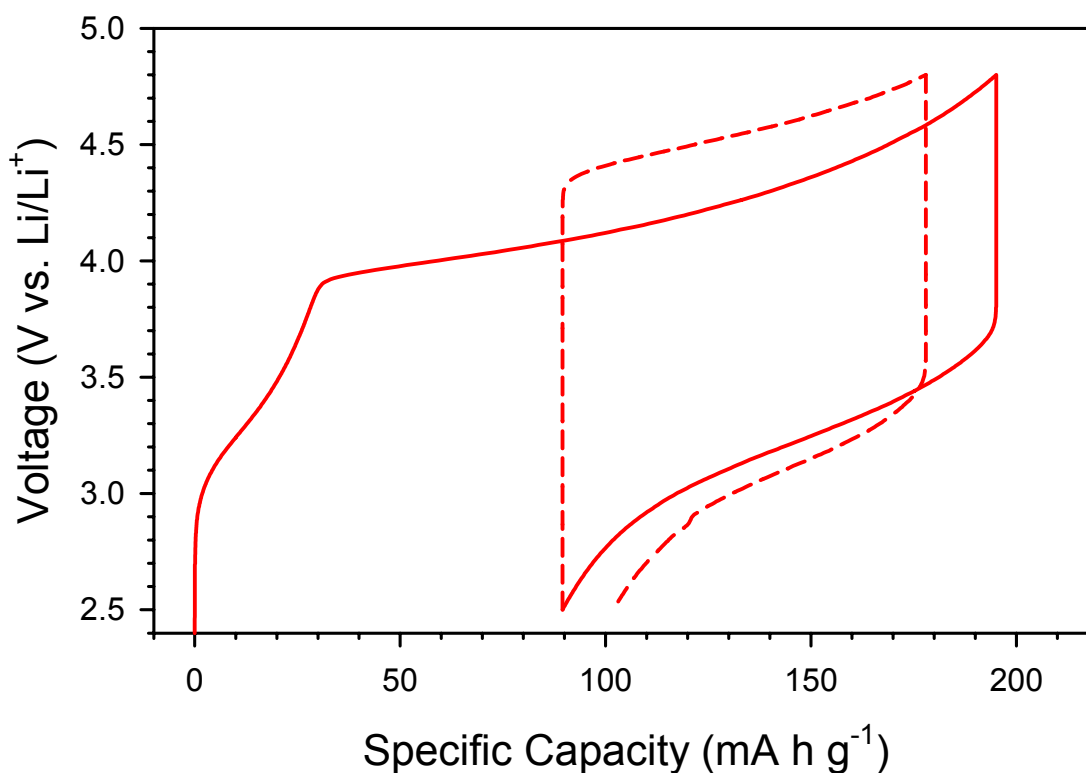


Figure 4. First and second charge-discharge curves for the electrochemical cell, $\text{Li}/\text{solid electrolyte}/\text{LiCoO}_2$ using ball milled $80\text{Li}_2\text{S}-20\text{P}_2\text{S}_5$. Irreversibility is caused by decomposition of solid state electrolyte.

Conclusion

Amorphous solid state electrolytes were prepared from high energy ball milling of the $[\text{xLi}_2\text{S}-(100-\text{x})\text{P}_2\text{S}_5]$ system. Electrolytes of the concentration $80\text{Li}_2\text{S}-20\text{P}_2\text{S}_5$ proved to

have the best overall performance, displaying an ionic conductivity on the order of 1×10^{-4} S cm⁻¹ at room temperature. Using cyclic voltammetry we found that heat treated glass-ceramic electrolytes exhibited better stability window characteristics than glass electrolytes of similar composition. Through X-ray diffraction we were able to observe key differences between samples of varying concentration and crystalline phase. The data obtained from XRD measurement provided validation for the conductivity responses taken from glass and glass-ceramic electrolytes. Because we found conductivity values in the glass-ceramic regime that reflected the trend of other works but not the values, an assessment of procedural differences would be in our best interest for future works. It is concluded that the solid state electrolyte 80Li₂S-20P₂S₅ glass-ceramic is the best candidate for use in lithium-ion secondary batteries.

Acknowledgments

This work has been supported by DARPA/DSO, Ms. Sharon Beermann-Curtin Program Manager, DARPA/DSO, and Michael F. Durstock, Ph.D. Air Force Research Lab.

References

1. A. Hayashi, S. Hama, F. Mizuno, *Solid State Ionics*, **175**, 683 (2004).
2. Y. Hashimoto, N. Machida, *Solid State Ionics*, **175**, 177 (2004).
3. M. Tatsumisago, *Solid State Ionics*, **175**, 13 (2004).
4. S. Kondo, K. Takada, Y. Yamamura, *Solid State Ionics*, **53**, 1183 (1992).
5. K. Takada, T. Inada, A. Kajiyama, *Solid State Ionics*, **158**, 269 (2003).
6. N. Machida, H. Yamamoto, S. Asano, *Solid State Ionics*, **176**, 473 (2005).
7. R. Mercier, J.-P. Malugani, B. Fahys, G. Robert, *Solid State Ionics*, **5**, 663 (1981).
8. A. Hayashi, H. Yamashita, *Solid State Ionics*, **148**, 381 (2002).
9. M. Tatsumisago, F. Mizuno, A. Hayashi, *J. Power Sources*, **159**, 193 (2006).
10. F. Mizuno, A. Hayashi, K. Tadanaga, *Solid State Ionics*, **177**, 2731 (2006).
11. F. Mizuno, A. Hama, A. Hayashi, *Chemistry Letters*, 1244 (2002).
12. H. Yamamoto, N. Machida, T. Shigematsu, *Solid State Ionics*, **175**, 707 (2004).
13. R. Kanno, M. Murayama, *J. Electrochem. Soc.*, **148**, A742 (2001).
14. A. Hayashi, S. Hama, H. Morimoto, *J. Am. Ceram. Soc.*, **84**, 477 (2001).